Acta Radiologica Open
6(11) 1–8

DOI: 10.1177/2058460117743279
journals.sagepub.com/home/arr
SAGE

CT Dental Artifact: Comparison of an Iterative Metal Artifact Reduction Technique with Weighted Filtered Back-Projection

Felix E Diehn[1], Gregory J Michalak[1], David R DeLone[1], Amy L Kotsenas[1], E Paul Lindell[1], Norbert G Campeau[1], Ahmed F Halaweish[2], Cynthia H McCollough[1] and Joel G Fletcher[1]

Abstract

Background: Dental hardware produces streak artifacts on computed tomography (CT) images reconstructed with the standard weighted filtered back projection (wFBP) method.

Purpose: To perform a preliminary evaluation of an iterative metal artifact reduction (IMAR) technique to assess its ability to improve anatomic visualization over wFBP in patients with dental amalgam or other hardware.

Material and Methods: CT images from patients with dental hardware were reconstructed using wFBP and IMAR software and soft-tissue or bone window/level settings. The anatomy most affected by metal artifacts was identified. Two neuroradiologists determined subjective and objective imaging features, including overall metal artifact score (1 = severe artifacts, 5 = no artifacts), soft-tissue visualization score of the most-compromised structure, and artifact length along the skin surface. CT numbers were used to quantify artifact severity.

Results: Twenty-four patients were included. IMAR improved overall metal artifact score in 18/24 cases (median = 2 ± 0.9 vs. 1 ± 0.6, $P < 0.001$). Mean CT number in the most-affected anatomical structure significantly improved with IMAR (94.6 vs. 219 HU, $P = 0.002$) and length of affected skin surface decreased (40.4 mm vs. 118.7 mm, $P < 0.001$). However, osseous/dental artifactual defects were found in 22/24 cases with IMAR vs. 11/24 with wFBP.

Conclusion: IMAR software reduced metal artifact both subjectively and objectively and improved visualization of adjacent soft tissues. However, it produced a higher rate of artifactual defects in the teeth and bones than wFBP. Our findings support the use of IMAR as a valuable complement to, but not a replacement for, standard wFBP image reconstruction.

Keywords
Metal artifact, dental artifact, artifact reduction, head and neck CT

Date received: 3 January 2017; accepted: 9 October 2017

Introduction

Computed tomography (CT) is a primary modality for diagnostic evaluation of the face and neck. A common limitation of CT in evaluating the soft tissues in and around the oral cavity is streak artifacts related to dental amalgam, which can obscure important anatomy and pathology. To minimize the impact of this artifact, a second CT is commonly acquired at a different gantry tilt angle, but this second acquisition is only routinely performed for certain CT protocols (such as soft-tissue neck CT at our institution), cannot be performed on CT systems unable to tilt the gantry

[1]Department of Radiology, Mayo Clinic, Rochester, MN, USA
[2]Siemens Healthcare, Malvern, PA, USA

Corresponding author:
Felix E Diehn, Mayo Clinic, 200 First Street SW, Rochester, MN 55905, USA.
Email: diehn.felix@mayo.edu

(such as the dual-source scanner used in the present study), adds radiation dose, and does not always prevent important structures from being concealed by artifacts.

Several investigators have proposed post-processing methods for decreasing the extent of metal-related artifacts in CT (1–9). Several of these publications have focused on the head and neck (1,8,9), comparing the current uncorrected clinical standard, weighted filtered back projection (wFBP) to linear interpolation metal artifact reduction, and iterative metal artifact reduction (IMAR).

In a study evaluating artifact reduction associated with spinal hardware (2), the use of an IMAR algorithm (Siemens Healthcare, Forchheim, Germany) minimized artifacts tangential to high-contrast regions on the basis of spatial frequency, recovering detail close to metallic objects. Thus, IMAR theoretically allows for retention of important anatomic information relative to the original images. In this study, we examined the extent to which IMAR would reduce hardware-related artifacts in soft tissues and osseous structures relative to wFBP and determined the extent to which it would improve diagnostic confidence among radiologists.

Material and Methods

Data collection and CT acquisition

Institutional review board approval was obtained and informed consent was waived for this retrospective study. All data were handled in a HIPAA-compliant manner. Imaging data were collected from 29 March 2013 to 1 October 2013. Inclusion criteria were: (i) non-contrast CT imaging of the temporomandibular joint (TMJ); (ii) presence of dental fillings and/or TMJ hardware; (iii) use of a 128-slice CT system (Definition FLASH; Siemens Healthcare); and (iv) archived CT projection data. Twenty-four patients met the inclusion criteria (age range = 21–79 years). The volume CT dose index ($CTDI_{vol}$) delivered was in the range of 14.3–42.1 mGy (mean $CTDI_{vol}$ = 17.7 mGy). In all cases, dental fillings were present, and in nine of the cases, TMJ hardware was also present in addition to dental amalgam (unilateral metal fossa implants in four, bilateral metal fossa implants in two, unilateral total TMJ prosthesis in two, and bilateral total TMJ prosthesis in one). All CT imaging was performed using our institution's routine clinical acquisition parameters for TMJ CT with a tube voltage of 120 kV, collimation of 128×0.6 mm, pitch of 0.6, gantry rotation time of 1 s, automatic exposure control tube current setting at 95 quality reference mAs (CareDose 4D, Siemens Healthcare), and a 30-cm scan field of view (FOV). TMJ CT imaging was evaluated because it is routinely performed on this specific non-tiltable gantry CT system at our institution; patients with TMJ hardware were therefore included in order to assess the performance of the algorithm in patients with implanted metal other than dental fillings.

Image reconstruction

CT images were reconstructed by a senior research technologist (GJM) from archived projection data using an offline computer workstation. Standard wFBP images were reconstructed using a conventional wFBP kernel (B40). The IMAR images were reconstructed using a prototype three-dimensional (3D) IMAR algorithm (see Kotsenas et al. (2) for a detailed description) and a B40 kernel. The IMAR algorithm is an iterative frequency split technique, which is designed to reduce blurring of the anatomical structures near the metal objects and to suppress the "streaking" that emanates from metal structures in CT images. For both wFBP and IMAR, images of 1-mm thickness at 0.5-mm increments were produced with a reconstruction FOV of 25 cm. IMAR was performed using a vendor-specified "dental" setting with predetermined IMAR reconstruction parameters appropriate for head and neck anatomy and hardware.

Image analysis

After reconstruction, images were loaded onto an Advantage Windows Workstation (GE Healthcare, Milwaukee, WI, USA) for viewing. Images were evaluated by both the principal investigator (PI) and by two additional readers (Fig. 1).

Selection of axial slice with subjectively worst artifacts by the PI: Before the reader study, each patient's wFBP images with soft-tissue window/level (W/L) settings (WW = 300 Hounsfield units [HU]; WL = 40 HU) were examined by the PI (a CAQ-certified neuroradiologist [FED] with five years of experience) to subjectively select the axial slice with the most metal artifacts. The position of this axial CT image was recorded, as was the anatomical structure that was most compromised by this artifact.

Subjective evaluation of metal artifacts by readers: For the reader study, two CAQ-certified neuroradiologists (DRD, ALK), each with 14 years of experience, evaluated images by consensus. At our institution, neuroradiologists interpret head and neck CT images, including TMJ examinations. The location and type of hardware were identified and recorded. Each study was evaluated by viewing axial wFBP and IMAR images side by side, first with soft-tissue W/L settings (WW = 300 HU; WL = 40 HU) and subsequently with bone W/L settings (WW = 3700 HU; WL = 600 HU).

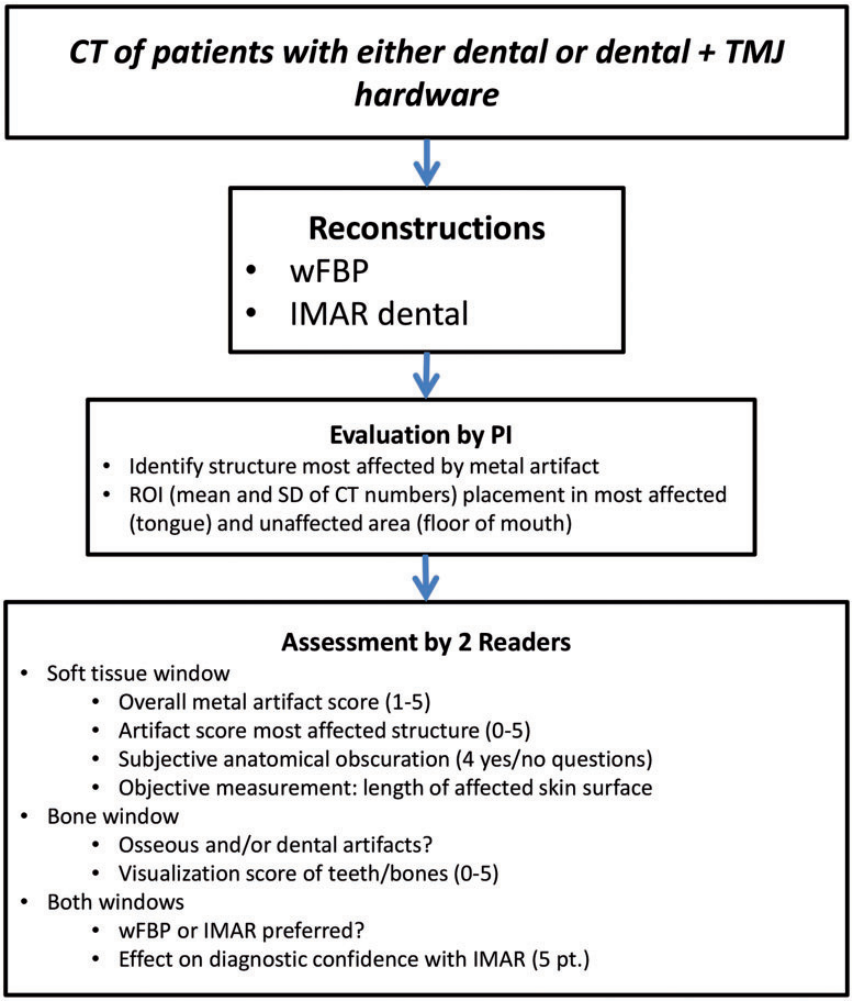

Fig. 1. Study flowchart showing PI and reader assessments of weighted filtered back-projection (wFBP) and iterative metal artifact reduction (IMAR) images using both subjective evaluation metrics and objective measurements. ROI, region of interest; TMJ, temporomandibular joint.

Side-by-side evaluation was chosen: (i) because the two techniques result in very different looking, subjectively identifiable images (making blinding impossible); (ii) to enable detection of any subtle potential differences between the two techniques; and (iii) so that artifacts introduced by the IMAR algorithm could be identified. Images were evaluated only in the axial plane without CT localizer radiograph (e.g. topogram) images or multiplanar reformations.

Using the soft-tissue W/L settings, the neuroradiologists assigned an overall metal artifact score based on their overall impression of soft-tissue planes and structures according to a five-point scale (1 = severe artifacts, not diagnostic; 2 = poor, partially non-diagnostic; 3 = moderate quality but limited confidence; 4 = good quality, diagnostic; 5 = excellent, no artifacts), similar to a previously reported scale (2). The neuroradiologists also examined the anatomic structure most compromised by the artifacts (identified by the PI, as above) and assigned a soft-tissue visualization score on a six-point scale (0 = totally obscured, no structures identifiable; 1 = marked artifacts, questionable recognition; 2 = faint anatomic recognition; 3 = anatomic recognition with low confidence; 4 = anatomic recognition with medium confidence; 5 = anatomic recognition with high confidence in a potential diagnosis), similar to a previously reported scale (2). Soft-tissue visualization scores were calculated by subtracting the score of the wFBP images from the score for the IMAR images, such that positive values reflected improvement with IMAR and negative values reflected degradation.

Subsequently, readers answered several yes/no questions about the extent of metal artifacts and how they affected the visualization of other anatomical structures:

1. Do any of the metal-related streak artifacts cross as a single, continuous line from the lingual (medial)

aspect of the mandibular cortex (gingiva) on the side of the metal to the lingual aspect of the contralateral side (rather than terminating in the oral cavity before reaching the contralateral mandible)?
2. Does the artifact reach the anterior aspect of the oropharynx (i.e. posterior to the oral cavity)?
3. Does the artifact reach the posterior aspect of the oropharynx (i.e. the posterior pharyngeal wall)?
4. Does the artifact reach the skin surface?

To evaluate images using the bone W/L setting, the readers examined the visualization of the teeth and bones near the metal implants. They identified any artifacts that obscured osseous or dental structures and described any bone or teeth that were compromised. They used the scale described above for the soft tissue to assign a visualization score for these artifactual defects.

For both W/L settings, the neuroradiologists subjectively evaluated image preference (wFBP preferred, IMAR preferred, or no preference) and estimated the overall impact of using IMAR vs. wFBP on diagnostic confidence using a 5-point scale (0 = unclear; 1 = probable increase; 10 = definite increase; –1 = probable decrease; –10 = definite decrease), similar to a previously reported scale (2).

Objective artifact evaluation by PI: The primary purpose of choosing a worst-affected region was to provide a region for the readers to evaluate in the above analysis. However, in order to objectively compare the amounts of streak artifacts between wFBP and IMAR images, we created regions of interest (ROIs) in this most-affected region and an unaffected control area. The PI drew a circular ROI that covered an area of 3.5–4 cm^2 entirely contained within the most-compromised anatomic structure. Another ROI of similar size was drawn in a subjectively unaffected area entirely within the floor of the mouth to use as an artifact-free reference. The location for this ROI was similar in each patient. The ROIs of both worst-affected and unaffected regions drawn in the wFBP images were copied and pasted into the IMAR images, in order to ensure that the exact same areas were examined in each image plane. The means and standard deviations (SDs) of the CT numbers in all of these ROIs were recorded and compared.

Objective artifact evaluation by readers: If the neuroradiologists identified artifacts that reached the skin surface using the soft-tissue W/L settings, they measured the length of the skin surface affected. Because no curvilinear measurement tool was available, this was done by determining the point at which the skin surface was affected and drawing connected line segments using a linear distance tool along the skin surface to the point at which the artifacts were no longer present. The total length of skin affected (in mm) was found by summing the distance covered by each line segment. A shorter length in the wFBP or IMAR image was considered a measure of artifact reduction.

Statistical analysis

The Wilcoxon signed-rank test was used to compare overall artifact degree, artifact degree in the worst structure, and artifact degree involving bone. Bowker's test for symmetry was used to evaluate the distribution of the overall metal artifact and artifact degree in worst anatomical structure scores for wFBP and IMAR. McNemar's test was used to compare the distributions of the binary variables evaluated in wFBP and IMAR images. Paired t-tests were used to compare the mean and SD in the ROIs drawn in the soft tissue with the worst artifacts and with no artifacts in the wFBP and IMAR images. The same test was used to compare the length of skin affected by the artifacts. A P value < 0.05 was considered statistically significant for all tests. Descriptive statistics were also used to summarize the number of cases in which artifact reached the skin surface, the number of cases in which IMAR introduced new artifacts in the bones/teeth, the subjectively preferred images in soft-tissue and bone W/L views, and the estimated impact on diagnostic confidence.

Results

In all cases, the PI identified the oral tongue as the worst-visualized structure. Even in cases with TMJ hardware, this was due to dental artifacts.

Subjective visualization of soft tissues (soft-tissue W/L)

The overall metal artifact scores were significantly higher for IMAR than for wFBP (Table 1). The improvement in overall metal artifact score was 1 in 18/24 cases (75%) and 0 in all others, with a mean of 0.75 ± 0.4.

The median soft-tissue visualization score for the tongue (the worst-visualized structure) was 0 ± 0.8 with wFBP (with a score of 0 indicating the structure is totally obscured), which improved to 1 ± 1.3 with IMAR (a score of 1 indicating marked artifacts, questionable recognition) ($P < 0.0001$). The mean improvement in this worst-visualized anatomical structure was 0.75 ± 0.7, with an improvement in 15/24 patients (63%) (Fig. 2). Bowker's test for symmetry showed evidence of asymmetry in both the overall artifact score ($P < 0.0001$) and soft-tissue visualization score in the worst-visualized anatomical structure ($P = 0.002$),

Table 1. Subjective and objective evaluation of wFBP and IMAR.

Neuroradiologist evaluation	wFBP	IMAR	*P* value
Subjective			
Overall soft-tissue artifact score	1 ± 0.6	2 ± 0.9	<0.001
Worst-affected soft-tissue visualization score	0 ± 0.8	1 ± 1.3	<0.001
Worst-affected bone visualization score	4 ± 1	2 ± 1.89	<0.001
Artifacts reached the skin surface	23/24 (96%)	15/24 (63%)	0.008
Artifacts crossed as a line between the mandibular lingual cortex (gingiva) to the lingual cortex (gingiva)	14/24 (58%)	17/24 (71%)	0.25
Artifacts reached both anterior and posterior aspects of the oropharynx	22/24 (92%)	22/24 (92%)	n/a
Artifactual dental/osseous defects, bone W/L	11/24 (46%) (3 dental, 7 osseous, 1 both)	22/24 (92%) (5 dental, 4 osseous, 13 both)	n/a
Subjectively better images, soft tissue W/L	0/24 (0%) Equal preference: 9/24 (37%)	15/24 (63%)	n/a
Subjectively better images, bone W/L	19/24 (79%) Equal preference: 5/24 (21%)	0/24 (0%)	n/a
Objective			
Mean CT number in affected area (HU)	219 ± 484	94.6 ± 75	Mean: 0.002 SD: < 0.001
Mean CT number in unaffected area (HU)	57 ± 25	57 ± 25	Mean: 0.82 SD: 0.82
Skin length affected by artifacts (mm)	118.7	40.4	< 0.001

wFBP, weighted filtered back-projection; IMAR, iterative metal artifact reduction; HU, Hounsfield units.

compatible with IMAR being superior to wFBP in both categories.

Subjective extent of artifact (soft-tissue W/L)

The artifacts reached the skin surface and were observed to cross as a single, continuous line from mandibular lingual cortex to lingual cortex (gingiva) more frequently in wFBP images than in IMAR images (Table 1); this difference was not statistically significant ($P = 0.25$). In 22/24 cases (92%), the artifacts reached the anterior and posterior aspects of the oropharynx with both IMAR and wFBP reconstruction.

IMAR artifacts involving teeth and bone (bone W/L)

In images viewed with bone W/L settings, artifactual defects within dental or osseous structures were identified in 22/24 cases (92%); 11/22 were in both the IMAR and wFBP images and 11/22 were in the IMAR images only (Fig. 3). The artifactual defects present in IMAR images were classified as dental in 5/22 cases (23%), osseous in 4/22 cases (18%), and both in 13/22 cases (59%). When present in wFBP images, they were classified as dental in 3/11 cases (27%), osseous in 7/11 cases (64%), and both in 1/11 cases (9%). The median visualization score for the worst-affected bone/teeth was 2 ± 1.89 for IMAR and 4 ± 1 for wFBP ($P < 0.0001$), with a mean improvement of -1.96 ± 1.49 (wFBP outperformed IMAR). In 20/24 cases (83%), the visualization score involving bone was worse in IMAR than wFBP, and in the remaining four cases there was no improvement.

Preference for IMAR or wFBP (soft-tissue and bone W/L) and impact on diagnostic confidence

When viewing the images in the soft-tissue W/L settings, IMAR was chosen as the subjectively better image in 15/24 cases (63%), and wFBP and IMAR were rated as equal in the remaining nine (Table 1). When viewing the images with the bone W/L settings, wFBP was chosen as the subjectively better image in 19/24 cases (79%), and wFBP and IMAR were rated as equal in the remaining five. The use of IMAR caused a probable increase in diagnostic confidence on the combination of soft-tissue and bone windows in 7/24 cases (29%), an unclear increase or decrease in 8/24 cases (33%), a probable decrease in 3/24 cases (13%), and a definite decrease in diagnostic confidence on the combination of soft-tissue and bone windows in 6/24 cases (25%).

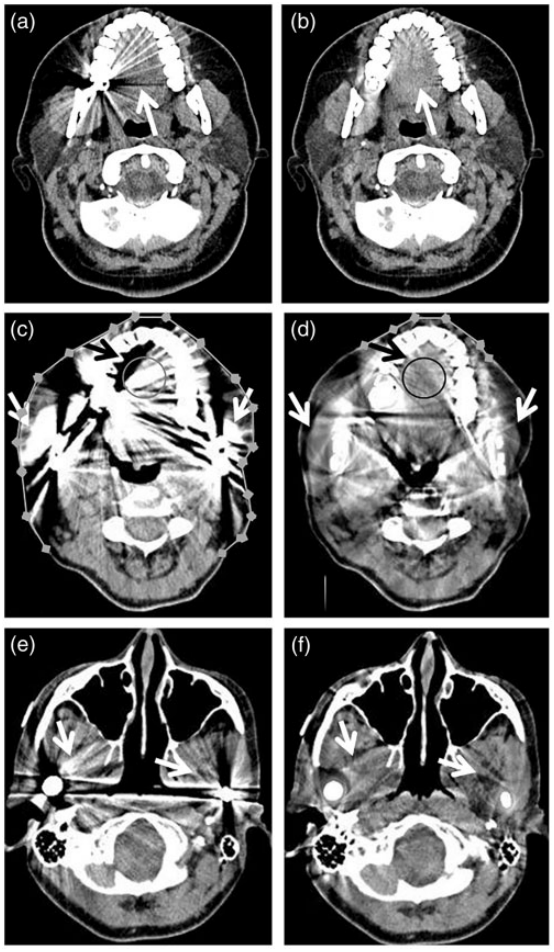

Fig. 2. Improved soft-tissue visualization with IMAR images. wFBP (left column, a, c, e) and IMAR (right column, b, d, f) images from two different patients: 41-year-old woman with dental fillings (a, b) and 54-year-old woman with dental fillings and bilateral mandibular hardware (c–f). The IMAR images (b, d, f) have reduced metal artifact compared with the wFBP images (a, c, e). This is particularly evident at the tongue (white arrows in (b) vs. (a), black arrows in (d) vs. (c)), the structure most affected by artifact in all 24 patients in this study. Samples of the circular ROIs drawn by the PI in the tongue are shown in (c, d); similar size ROIs were also drawn in unaffected regions within the floor of the mouth (more inferiorly) to serve as artifact-free reference for HU measurements (not shown). In this example, the mean CT number at the tongue on the wFBP image (c) was 204 HU, much higher than on the IMAR image (d), 97 HU. Additional objective artifact evaluation involved readers drawing multiple connected line segments to measure the length of skin affected by artifact (c, d). In this example, the length of skin affected by artifact was much longer on the wFBP image than the IMAR image, 264 mm vs. 55 mm. The soft tissues adjacent to the bilateral mandibular hardware (white arrows in c–f) are also much less affected by artifact in the IMAR (d, f) than the wFBP (c, e) images.

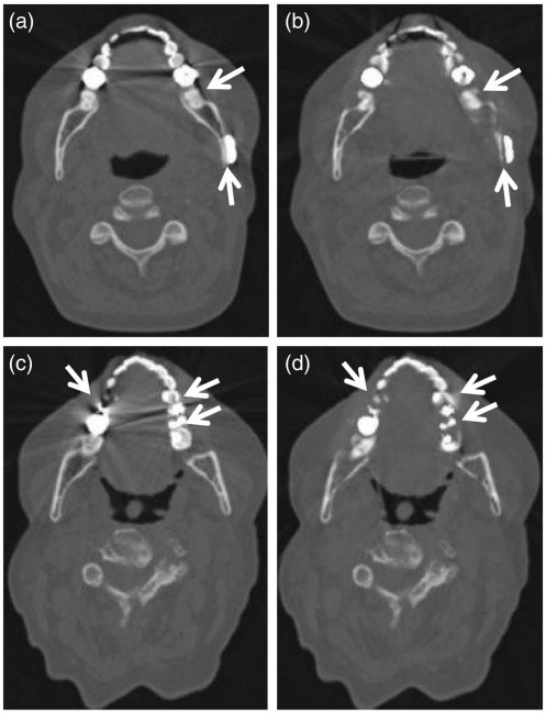

Fig. 3. Artifactual defect introduction in IMAR images reconstructed with bone window/level settings. wFBP (left column, a, c) and IMAR (right column, b, d) images from two different patients: 53-year-old woman with dental fillings and mandibular hardware (a, b) and 69-year-old woman with dental fillings (c, d). The IMAR images (b, d) introduce artifactual defects along teeth and adjacent bone compared to the wFBP images (a, c) (arrows, a–d). These defects can be seen adjacent to both teeth (b, d) and mandibular hardware (posterior arrow in (b)).

Objective measurements of artifact (soft-tissue W/L)

The mean CT numbers (and associated SDs) were identical in the unaffected areas, but were much higher in the wFBP images than in the IMAR images in the affected areas (Table 1), indicating less artifact in the IMAR images. The skin surface covered by metal artifacts was also much longer in the wFBP images than the IMAR images (Table 1).

Discussion

The current study demonstrates that IMAR, relative to wFBP, can subjectively and objectively improve image quality of soft tissues in head/neck CT images by reducing dental streak artifacts, but at the cost of introducing some osseous/dental artifacts near dental amalgam and other metallic implants. These results are important because dental amalgam is ubiquitous,

and obscuration of anatomy and pathology by dental streak artifacts is a major limitation of CT of the soft tissues of the head and neck. IMAR does not yield additional radiation dose, as does for example a second re-angled CT acquisition, which is currently a commonly employed technique. The osseous/dental structures near amalgam are intact on wFBP images, but without this knowledge, such IMAR-related artifacts could be clinically misinterpreted as osseous erosion in patients with head and neck malignancy. Thus, in its current form IMAR is a complement to wFBP, with the former comparatively improving visualization (and reader preference) of soft tissues and decreasing visualization (and reader preference) of bones and teeth.

Several other studies have examined artifact reduction with IMAR, using either two-dimensional (2D) or 3D versions. Our results confirm the work of Weiss et al., which demonstrated IMAR's significant artifact reduction and improved visualization of anatomic structures adjacent to dental fillings in a similarly sized study sample (8). However, their publication analyzed a 2D version of IMAR, while we report on a 3D prototype version which also corrects in the z-direction. Wuest et al. found that 3D IMAR yielded higher image quality than wFBP and linear interpolation metal artifact reduction and, as in our study, noted that IMAR introduced artifactual defects near teeth and adjacent osseous structures (9). Unlike either of these prior studies, we included objective measures of the amount of artifact, such as the length of skin surface affected. We also qualitatively evaluated the most-affected anatomic structure and how far the artifact extended across oral structures, providing more points of comparison.

Our study and those of Wuest et al. and Weiss et al. (8,9) analyzed IMAR algorithms from the same vendor. De Crop et al. reported on a different vendor's metal artifact solution in the oral cavity in a cadaveric/phantom study, but one of the two algorithms assessed (model-based iterative reconstruction) is primarily designed for image denoising rather than metal artifact reduction (1). Several other recent studies have assessed metal artifact reduction related to dental amalgam, but these are all based on phantom work (10–13). Cha et al. performed a study of the impact of metal artifact reduction software on dental artifacts with a similar number of participants to our present investigation (14). This investigation used dual-energy CT rather than a conventional single-energy CT protocol and a non-iterative algorithm. In their study, the artifact reduction software also significantly reduced metallic dental artifacts both subjectively and objectively, including in the tongue.

Because this was a preliminary investigation of a new technique, several aspects of our study may limit the ability to generalize the results. First, readers were not blinded to the reconstruction method. We chose this side-by-side approach in order to allow detection of any subtle differences between the two techniques and identification of artifacts introduced by the IMAR algorithm. In addition, the differences in appearance of the two techniques make blinding difficult to achieve. Image review was conducted by consensus rather than independent analysis, in part to match prior published work on IMAR (2). The chosen CT scan type was a non-contrast TMJ protocol maxillofacial CT, and we did not extend the evaluation to other types of protocols, such as contrast-enhanced exams. Furthermore, the CT images were only evaluated in the axial plane, and not in the coronal or sagittal planes as they would typically be clinically. Additionally, the artifacts were primarily due to dental fillings, and given the heterogeneity of filling composition, an analysis of artifact severity with respect to specific metal was not feasible. Finally, the sample size was small; however, given the high degrees of statistical significance for the main results and the clear subjective difference between the two reconstruction techniques, it is unlikely that a larger sample size would result in substantially different results.

The present study did not evaluate the performance of the IMAR algorithm in oromaxillofacial diseases, in part because at our institution clinical soft-tissue neck CT examinations are currently not performed on the chosen CT platform. However, in future work, we will examine the clinical relevance of using IMAR by evaluating pathology as well as anatomy in clinical cases involving confirmed conditions such as neoplasm or dental infection in the oral cavity or pharynx. The reconstruction with the 3D IMAR algorithm was performed on an off-line computer workstation; the associated significant delay in workflow, which would preclude the routine clinical use of IMAR, was not measured. A less time-intensive 2D version of IMAR is now clinically available by the vendor platform used in this study and under current investigation. If the current results are upheld, IMAR could provide increased sensitivity and improved diagnostic confidence over wFBP when identifying these pathologies.

In conclusion, the IMAR reconstruction technique reduces dental artifacts both subjectively and objectively and improves visualization of soft-tissue anatomy in the oral cavity and oropharynx. However, these

benefits are accompanied by a major limitation compared to wFBP—introduction of nearby artifacts within the teeth and bone. At present, the use of both IMAR and wFBP images provides optimal visualization in critical head and neck structures compromised by dental amalgam artifact.

Acknowledgements

The authors thank Adam Bartley for his statistical contribution, Naomi Ruff for her assistance with manuscript editing, and Kristina Nunez for her assistance with manuscript preparation.

Declaration of conflicting interests

The author(s) declared the following conflicts of interest with respect to the research, authorship, and/or publication of this article: Dr. McCollough receives industry grant support from Siemens Healthcare. Dr. Halaweish is an employee of Siemens Healthcare. All other authors declare that there is no conflict of interest.

Funding

The author(s) disclosed receipt of the following financial support for the research, authorship, and/or publication of this article: Software was provided for this work from Siemens Healthcare. Partial research funding for this work was provided by a grant from Siemens Healthcare.

References

1. De Crop A, Casselman J, Van Hoof T, et al. Analysis of metal artifact reduction tools for dental hardware in CT scans of the oral cavity: kVp, iterative reconstruction, dual-energy CT, metal artifact reduction software: does it make a difference? Neuroradiology 2015;57:841–849.
2. Kotsenas AL, Michalak GJ, DeLone DR, et al. CT metal artifact reduction in the spine: can an iterative reconstruction technique improve visualization? Am J Neuroradiol 2015;36:2184–2190.
3. Lee YH, Park KK, Song HT, et al. Metal artefact reduction in gemstone spectral imaging dual-energy CT with and without metal artefact reduction software. Eur Radiol 2012;22:1331–1340.
4. Lell MM, Meyer E, Schmid M, et al. Frequency split metal artefact reduction in pelvic computed tomography. Eur Radiol 2013;23:2137–2145.
5. Meinel FG, Bischoff B, Zhang Q, et al. Metal artifact reduction by dual-energy computed tomography using energetic extrapolation: a systematically optimized protocol. Invest Radiol 2012;47:406–414.
6. Meyer E, Raupach R, Lell M, et al. Normalized metal artifact reduction (NMAR) in computed tomography. Med Phys 2010;37:5482–5493.
7. Meyer E, Raupach R, Lell M, et al. Frequency split metal artifact reduction (FSMAR) in computed tomography. Med Phys 2012;39:1904–1916.
8. Weiss J, Schabel C, Bongers M, et al. Impact of iterative metal artifact reduction on diagnostic image quality in patients with dental hardware. Acta Radiol 2017;58: 279–285.
9. Wuest W, May MS, Brand M, et al. Improved image quality in head and neck ct using a 3D iterative approach to reduce metal artifact. Am J Neuroradiol 2015;36: 1988–1993.
10. Funama Y, Taguchi K, Utsunomiya D, et al. A newly-developed metal artifact reduction algorithm improves the visibility of oral cavity lesions on 320-MDCT volume scans. Phys Med 2015;31:66–71.
11. Hegazy MA, Cho MH, Lee SY. A metal artifact reduction method for a dental CT based on adaptive local thresholding and prior image generation. Biomed Eng Online 2016;15:119.
12. Huang JY, Kerns JR, Nute JL, et al. An evaluation of three commercially available metal artifact reduction methods for CT imaging. Phys Med Biol 2015;60: 1047–1067.
13. Wagenaar D, van der Graaf ER, van der Schaaf A, et al. Quantitative comparison of commercial and non-commercial metal artifact reduction techniques in computed tomography. PLoS One 2015;10:e0127932.
14. Cha J, Kim HJ, Kim ST, et al. Dual-energy CT with virtual monochromatic images and metal artifact reduction software for reducing metallic dental artifacts. Acta Radiol 2017;58:1312–1319.